# The formation of explosive volcanos at the circum-Pacific convergent margin

**Wei-Dong Sun** ( weidongsun@qdio.ac.cn )
Center of Deep Sea Research, Institute of Oceanology, Chinese Academy of Sciences, Qingdao 266071
https://orcid.org/0000-0002-9003-9608

**Fanfan Tian**
Center of Deep Sea Research, Institute of Oceanology, Chinese Academy of Sciences, Qingdao 266071

**Kun Wang**
Center of Deep Sea Research, Institute of Oceanology, Chinese Academy of Sciences, Qingdao 266071

**Guozhi Xie**
CAS Key Lab of Marine Geology and Environment, Center of Deep Sea Research, Institute of Oceanology, Chinese Academy of Sciences, Qingdao 266071

**Physical Sciences - Article**

**Keywords:**

**Posted Date:** March 18th, 2022

**DOI:** https://doi.org/10.21203/rs.3.rs-1407913/v1

# The formation of explosive volcanos at the circum-Pacific convergent margin

Fanfan Tian[1-3†], Kun Wang[1-3†], Guozhi Xie[1-3†], Weidong Sun[1-3*]

[1] Center of Deep Sea Research, Center of Ocean Mega Science, Institute of Oceanology, Chinese Academy of Sciences, Qingdao 266071, China

[2] Laboratory for Marine Geology, Qingdao National Laboratory for Marine Science and Technology, Qingdao 266237, China

[3] University of Chinese Academy of Sciences, Beijing 100049, China

*__Corresponding author:__ weidongsun@qdio.ac.cn

† Equally contributed

**Abstract: The circum-Pacific convergent margin is known as "the Ring of Fire", with abundant volcano eruptions[1]. Gigantic eruptions are rare but very disastrous. It remains obscure how are large disastrous volcanos formed[2,3] and where are the danger zones[4-6] in the near future. Here we show that the three largest eruptions since 1900, the Hunga Tonga-Hunga Ha'apai, the Mount Pinatubo and the Novarupta volcanos, are all associated with subductions of volatile rich sediments and slab windows in the subducting plate underneath. Among them, the newly erupted Hunga Tonga-Hunga Ha'apai volcano is closely concomitant with the subduction of the Louisville Seamount Trail, whereas the Mount Pinatubo volcano is right next to the subducting fossil ridge of the South China Sea. Both seamount chains have water depths much shallower than the carbonate compensation depths in the Pacific Ocean. The water depths of the Pacific plate subducting underneath the Novarupta volcano are also shallower than the carbonate compensation depths. Therefore, these subducting slabs contain abundant carbonates. Slab windows expose the mantle wedge directly to the hot asthenosphere, which increases the temperature and dramatically promotes the partial melting of the carbonate-fluxed mantle wedge, forming volatile-rich magmas that powered explosive eruptions. Slab window and subduction of carbonate are the two most important favorable conditions for catastrophic eruptions. Considering that the Mount Fuji meets both criteria, it may be classified into a danger zone for catastrophic volcano eruptions.**

On January 15, 2022, the Hunga Tonga-Hunga Ha'apai (HTHH) volcano (20.536°S, 175.382°W, Fig. 1a-b) erupted violently in the Kingdom of Tonga, southwest Pacific, reaching the volcano eruption index of 5. It is the largest volcanic eruption in the last 30 years. The circum-Pacific region is known as the Ring of Fire, with abundant volcanic eruptions. Gigantic eruptions are usually catastrophic. For examples, both the Mount Pinatubo and the Novarupta volcanos (Fig. 1c-d) have resulted in major climate changes[7-10]. What controlled the formation of gigantic volcanos? Where are the danger zones of catastrophic eruptions? These questions are of critical importance to the human society, but yet remain essentially untouched. Here we show that slab windows and the subduction of carbonate are the two prerequisites for gigantic explosive eruptions

**Volatiles in the HTHH volcano**

The HTHH volcano has erupted ca. 5 cubic kilometers of volcanic ash and tephra, with abundant $CO_2$ but only 0.4 megatons of $SO_2$. To produce magmas with such a low $SO_2$, the mantle source should have sulfur contents of less than 20 parts per million. The average sulfur abundance in the upper mantle is about 250 parts per million[11]. This means that the mantle source of the HTHH volcano is highly depleted in sulfur.

Sulfur is a highly incompatible element under the oxygen fugacity of convergent margin magmas. Therefore, previous partial melting can dramatically depress the sulfur contents in the volcano. In a well-developed arc, like the Tonga arc, the sulfur content in the mantle wedge is lower than that of the upper mantle. However, $CO_2$, water, and other volatiles are also highly incompatible during partial melting. Therefore, a highly

depleted mantle source is usually also depleted in volatiles. However, the explosive eruption of the HTHH volcano indicates high volatile contents, e.g., $CO_2$.

Tectonically, the HTHH volcano is located on the Tonga-Kermadec trench (Fig. 1a), which is well known for gigantic eruptions[12-14]. As an intra-oceanic subduction zone far away from continents, the Pacific plate subducting underneath Tonga is lack of sediments, with a total sediment thickness of <100 meters[15]. The water depths of the Pacific plate to the east of the Tonga trench is >5000 meters[16], which is deeper than the carbonate compensation depths (CCD, 4500 m) of the Pacific Ocean[17]. Therefore, not much carbonate is expected in the sediments. However, the carbon isotopes of arc volcanic rocks in this region show clear carbonate recycling characteristics[18]. This was attributed to carbonate from the altered oceanic crust[18].

**The subduction of the Louisville Seamount Trail**

The remnant of the Louisville Seamount Trail is ca. 75 km wide and 4500 km long, which is located exclusively to the south of the Osbourn Trough. It is a typical plume tail formed by the eruption of the Louisville mantle plume. The Osbourn Seamount, which is now located close to the trench, is the oldest seamount that has not been subducted yet in this trail. It erupted right next to the fossil spreading center of the Osbourn Trough (Fig. 2), at 76.7 Myrs ago[19].

The Osbourn Trough is a fossil ridge formed after the eruption of the Ontong Java Plateau at ~ 119-125 Ma[20,21], and was abandoned at ~ 86 Ma[22], when the ridge jumped further south[23,24]. This indicates that seamounts of the Louisville Seamount Trail older than 77 Myr erupted either on or to the north of the Osbourn Trough. Considering that

the Osbourn Trough was spreading before 86 Myr, all the Louisville seamounts older than 86 Myr were once carried further north from the Osbourn Trough (Fig. 1a).

The HTHH volcano is located right above the subduction pathway of the Louisville Seamount Trail ca. 3 million years ago (Fig. 2). Plate reconstruction shows that the Louisville Seamount Trail started to subduct from the northeast corner of the Tonga Arc, and migrated southward[25]. The Osbourn Trough is currently subducting towards ca. 300° at ca. 25.5° S. The Louisville Seamount Trail is pointing towards 336°, i.e., the angle between it and the Tonga subduction zone is about 36° (ref. 25).

The north end of the Tonga subduction zone is the fastest convergent plate boundary in the world, with subduction a rate of 240 km/Myr[26], which declines southwestward. This is likely due to the collision of the Louisville Seamount Trail with the Tonga Arc. Consistently, the Tonga Arc is clear curved westward at ~23.5°S, which marks the location of the latest collision/subduction. The northwestward drifting rate of the Pacific plate is ca. 70 km/Myr, whereas the opening of the Lau Basin in the middle of the Tonga Arc is ca. 60 km/Myr[26], i.e., the subduction rate is ca. 130 km/Myr.

The distance between the Tonga trench and the HTHH volcano, is about 360 km. Seismic results show that the depth of subducting slab beneath the HTHH volcano is about 80 km. Hence, at a subduction rate of 130 km/Myr, it takes ca. 3 million years for the subducting seamounts to reach the location underneath the HTHH volcano. As illustrated in Fig. 3, there should be subducted Louisville seamounts near the mantle source of the HTHH volcano.

Compared with altered oceanic crust with water depths deeper than the CCD, the

Louisville Seamount Trail is more abundant in carbonate. It consists of many individual seamounts of 30-75 km in diameters[27] and 2865-4480 m in elevation from the seafloor. The water depths of the top of these seamounts are 250-1920 m, which are much shallower than the CCD, such that carbonate is stable on these seamounts. This is supported by IODP Expedition 330 drill cores[27].

The Louisville mantle plume is located at ca. 50° S. In general, the coral reef is not popular at such high latitude. However, one drill hole recovered ~15 m thick algal limestone reef, whereas the other three drill holes also recovered several condensed pelagic limestone intervals of up to 30 cm thick and multiple layers of foraminiferal sand interlayered with lava and carbonate-cemented volcanic breccia[27]. Seamounts drilled by IODP Expedition 330 all erupted before the warm period in the early Cenozoic, when the global temperature was up to 5-15 °C higher than that in the late 20th century[28], such that limestone reefs may form at high latitudes during this period. Nevertheless, nummulitic limestone samples have been dredged from Burton Guyot in the Louisville Seamount Trail, which indicates the presence of Eocene shallow-water reef in the high- to mid-latitude Pacific[27].

The Louisville guyots were originally islands high above sea level[27]. All the drill holes of IODP Expedition 330 were put on the flat top of different guyots, and yet the drill hole samples have erupted at shallow water depths and even subaerially, with erosional unconformities[27]. The diameter of the flat top of these guyots ranges between 5-15 kilometers[29], suggesting that islands were originally thousands of meters above sea level, the deplanation of which took a long time. These guyots were possibly formed

even after the early Cenozoic warm period. Therefore, drill holes on the flat top of these guyots are not representative in term of reefs. The hillsides may have much thicker limestone reefs.

Carbonates on the seamounts of the Louisville Seamount Trail are well protected by the interlayered lava. The subduction of these seamounts may carry a large amount of carbonate into the mantle wedge[18].

Carbonate may lower the solidus temperature of mantle peridotite by up to ca. 300 °C[30]. Therefore, the subduction of the seamounts is favorable for the formation of gigantic volcanos. More importantly, it provides $CO_2$ that charge the magma chamber and powered the explosive eruptions.

The distribution of earthquakes shows that the subducting Pacific plate was torn apart underneath this region, forming slab windows[31]. In addition to the slab window roughly perpendicular to the trench, the slab underneath the HTHH volcano is also torn (Extended Data Fig. 1), forming a slab window roughly parallel to the trench, which is likely responsible for a new volcano line behind the Tonga Arc, the Tofua Arc. The HTHH is one of them.

These slab windows expose the cold mantle wedge to the hot asthenosphere mantle, resulting in abnormally high temperatures. The subduction of shallow seamounts and slab windows together, endorse the formation of volatile-rich gigantic volcanos. Based on these criteria, volcano “A” further to the south on the Tofua arc volcanic chain (Extended Data Fig. 3) is more dangerous than the HTHH volcano.

**The Mount Pinatubo eruption**

The Mount Pinatubo is the largest volcano in the last 100 years. It erupted in 1991 on the Luzon Island, the Philippines (120.35°E, 15.13°N, Fig. 1b). The Mount Pinatubo volcano is classified as volcano eruption index of 6, with a total eruption volume of 8.4 to 10.4 cubic kilometers, including about 5-6 and 3.4-4.4 cubic kilometers of ignimbrite and fallout deposits, respectively[8]. About 15-20 megatons of $SO_2$ were ejected up to 40 kilometers high, into the stratosphere[8]. It has cyclical eruptions, which is the same with HTHH volcano. The last major eruption occurred in A.D. 1500 with roughly the same size as those of 1991[9].

Similar to the HTHH volcano, the Mount Pinatubo volcano is also associated with seamount subduction and a slab window nearby (Fig. 1b). It is located at the convergent margin in the west Philippines, where the fossil ridge of the South China Sea subducting underneath the Luzon Island[32]. Seismic imagines show that the ridge subduction formed a slab window[33].

The fossil ridge of the South China Sea consists of large seamounts, with thick coral reefs. Among them, the Huangyan Island is the largest one. The subduction of this fossil ridge has been carrying down a large amount of carbonate since ca. 15.5 Ma ago[34]. The oldest eruption identified in the Mount Pinatubo is 1.1 Ma[9], likely after the opening of the slab window.

The main difference between the Mount Pinatubo and the HTHH volcanos is that the former is close to the continent with a large amount of sediments subducting alongside the ridge. Therefore, far more sulfur has been released in the Mount Pinatubo volcano, which had a major influence on the climate[35].

**The Novarupta volcano**

The Novarupta volcano (Fig. 1c) is the largest volcano in the 20th century. It erupted in 1912 with a total output of ~28 cubic kilometers, including at least 17 cubic kilometers of fall deposits and about 11 cubic kilometers of ash-flow tuff [7]. It is volatile rich and had a major influence on global climate[7,36].

The Novarupta volcano is located at the end of the Alaska Peninsula, whereas the Pacific plate is subducting northwestward along the Aleutian-Alaska trench. The average water depths of the Pacific plate to the southeast of the Aleutian-Alaska trench is shallower than the CCD[16] (Fig. 1c). There are thick sediments covering on the ocean floor and seamounts. The subducting sediments of the Aleutian-Alaska trench are more than 350 m thick, comprised of carbonates, interlayered with pelagic clay, ashy-siliceous clay and turbidites[37,38]. Seismic data also shows that there are slab windows nearby[39] (Extended Data Fig. 2). Once again, both sediments and slab window are favorable for the formation of this gigantic volcano.

**The Mount Fuji**

The Mount Fuji (Fig. 1d), Japan, is another large volcano in the circum-Pacific region, which is 3775.63 meters above sea level, covering an area of 1200 $km^2$. It has erupted 4 times in since A.D. 800. However, all these eruptions were quite small compared to the HTHH volcano. Tectonically, the Mount Fuji is located near the junction of the subducting Pacific and the Philippine Sea plates, and the Japan and the Izu-Bonin-Mariana Arcs. The water depths of the Pacific plate subducting near the Mount Fuji are much deeper than the CDD. Carbon recycling in the northwest Pacific

is dominated by organic carbon in black shales. However, the Izu-Bonin-Mariana back arc basin plate, together with its spreading ridge and arcs, is subducting towards the Mount Fuji at a rate of 5-6 cm/year[40,41]. The spreading ridge of the Izu-Bonin-Mariana back arc basin has an average water depth of ~ 2600 meters[42], which is far shallower than the CCD [17]. Therefore, there should be carbonate on the ridge. Previous seismic study has indicated a clear gap, i.e., a slab window, just beneath the Mount Fuji[43]. These suggest that the next major eruption of the Mount Fuji could be catastrophic.

**Concluding remarks**

The water depths of the west Pacific plate are usually deeper than the CCD. Therefore, seamount subduction is the most favorable process that forms violent gigantic volcanos. Subducted seamounts with water depths shallower than the CCD provide carbonates that enhance the melting capacity of the mantle wedge and release carbon dioxides that drive explosive eruptions. Slab windows nearby is another key factor, which elevates temperatures and increase the melting capacity of the mantle wedge.

In the case of Tonga, subducted carbonate has very low sulfur contents, much lower compared to sediments of continental origin. Meanwhile, cyclical gigantic eruptions have purged sulfur out of the source, resulting in the cleanest gigantic volcanic eruption ever reported. For gigantic volcanos associated with the subduction of continental sediments, e.g., the Mount Pinatubo and the Novarupta volcanos, sulfur contents are usually much higher and more catastrophic.

## Methods

**Detrital seismic data compilation.** We used the generic mapping tools (GMT) to draw the topography and bathymetric map of the study regions. The seismic data in study regions are from the ISC-EHB catalog, which is a groomed version of the ISC Bulletin and contains thousands of seismic events from 1964 to 2018[44]. We counted and plotted the locations of the seismic event with $M_b > 5$ for the Tonga region and $M_b > 4$ for the Novarupta region (Extended Data Fig. 1-2). Seismicity in the vertical section is the distribution of events along with a sideline 20 km wide for both Hunga Tonga-Hunga Ha'apai volcano and Novarupta volcano region. We found the slab tearing in both regions, which is the important condition for the catastrophic eruption.

**Details of Hunga Tonga-Hunga Ha'apai volcanic eruption.** We studied the details of Hunga Tonga-Hunga Ha'apai volcanic eruption by collecting the latest reports[12-14] and volcanic databases of the volcano[45].

**Volcano, seamount and water depth data.** A sufficient quantity of representative volcano, topographic and bathymetric data now exists to chronicle the catastrophic eruption, seamount and water depth data over time. Volcano, seamount and water depth data from previous studies have here been collected and used to verify our study from different databases, including the Global Volcanism Program[45], the Seamount Catalog[46] and Bathymetric Data Viewer[16]. The water depths of Pacific ocean, calcite compensation depth and Tonga trench used in the main text are from Encyclopedia Britannica[17,47,48] and Bathymetric Data Viewer[16].

## Data availability

The sources of all data are available in the manuscript or the supplementary materials.

## Acknowledgements

We thank R. J. Arculus, whose encouragement and suggestions greatly improved the early versions of the manuscript. This work was supported by the Strategic Priority Research Program of the Chinese Academy of Sciences (XDA22050103), the Taishan Scholar Program of Shandong (ts201712075).

## Author contributions

W.D.S. initiated the idea and drafted the manuscript. F.F.T. and K.W. plotted most of the figures. G.Z.X. edited the main text and the supplementary. All authors contributed to interpreting data and revising the manuscript.

**Competing interests:** The authors declare no competing interests.

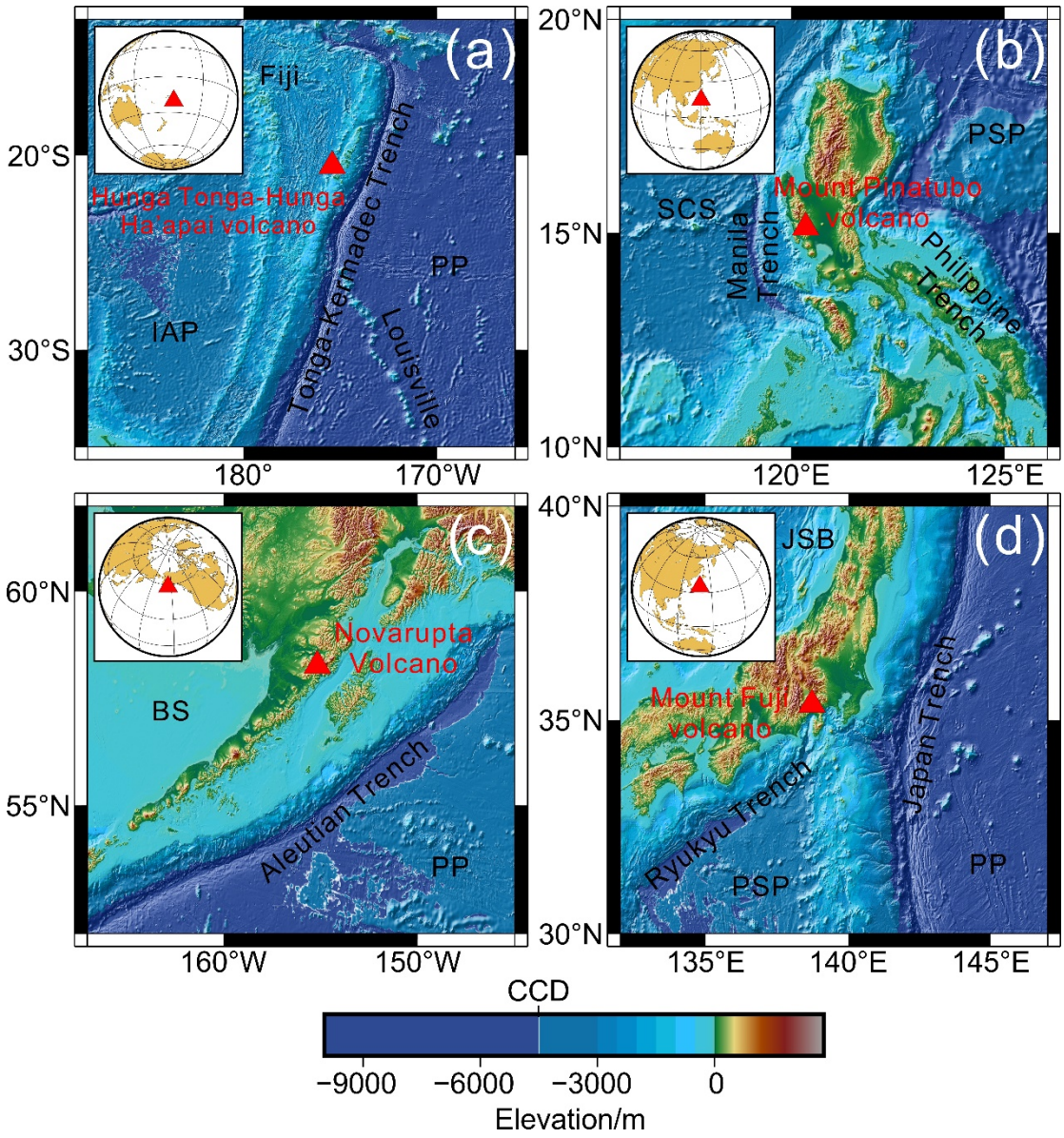


**Figure 1 | Overview of gigantic volcanos in the circum-Pacific region.** The locations of the Hunga Tonga-Hunga Ha'apai, the Mount Pinatubo, the Novarupta and the Mount Fuji volcano (red triangle). (a)-(d) Topography and bathymetric map of the Hunga Tonga-Hunga Ha'apai, the Mount Pinatubo, the Novarupta and the Mount Fuji volcano regions in the Pacific using GMT [49]. PP, Pacific Plate; IAP, Indo-Australian Plate; PSP, Philippine Sea Plate; SCS, South China Sea; BS, Bering Sea; JSB, Japan Sea Basin. All these gigantic explosive eruptions are associated with subduction of geologic units higher than CCD, e.g., seamounts or ridge.

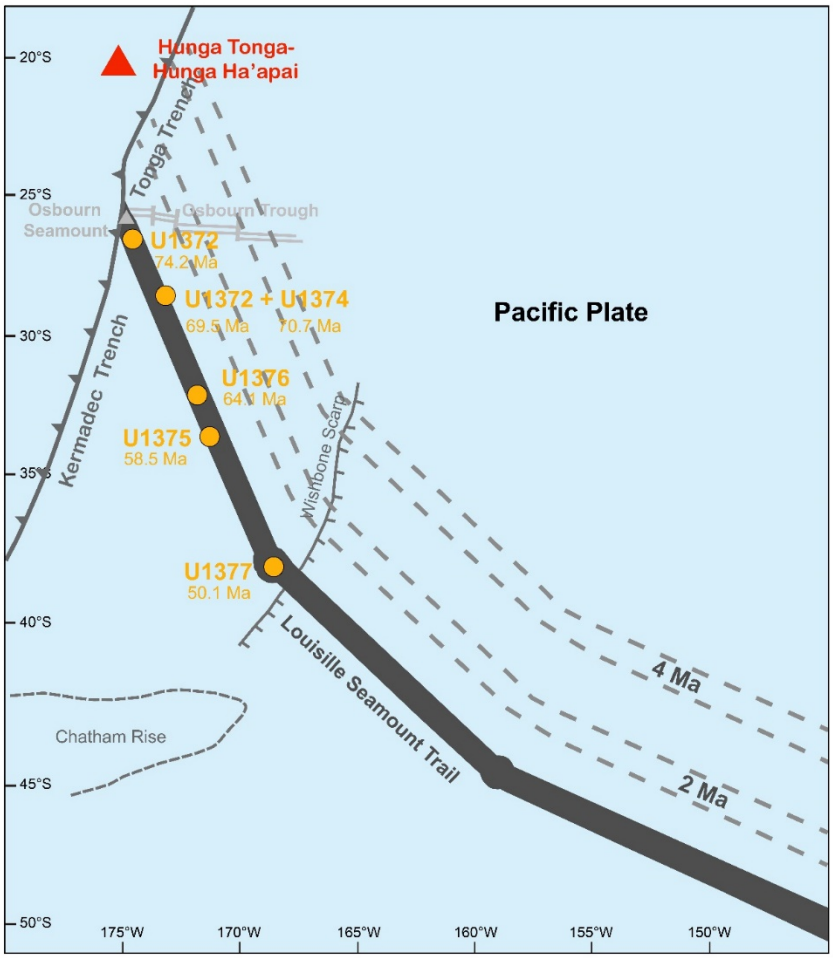


**Figure 2 |** The subduction history of the Louisville Seamount Trail[25,27]. It started to subduct from the northeast corner of the Tonga Arc and was migrating fast towards the southwest. The indentation of the Tonga Arc at ~ 23.5 °S marks the collision between the Louisville Seamount Trail and the Tonga Arc. It was subducting towards the HTHH volcano ca. 3 Ma ago, and thus there should be subducted seamounts underneath the HTHH volcano, providing $CO_2$ that powered explosive eruptions.

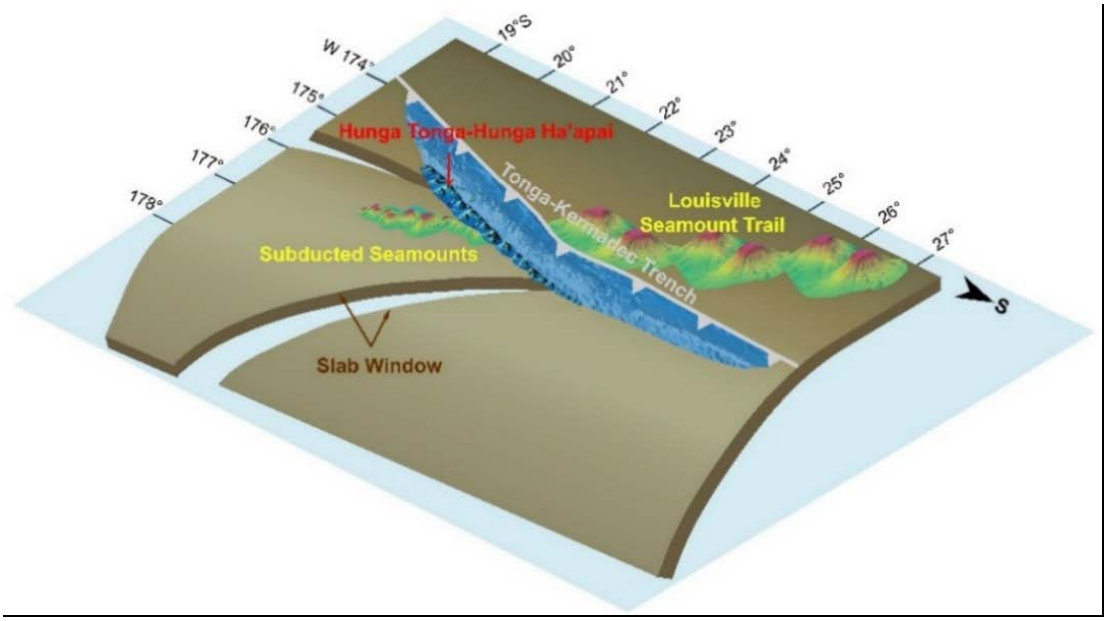


**Figure 3 | The eruptions of HTHH volcano caused by Ridge subduction coupled with slab window.** A cartoon illustrating that ridge subduction coupled with slab window is favorable for the formation of gigantic eruptions of the HTHH volcano. The Tofua arc volcano line behind the main island of Tonga is associated with a shallower slab window parallel to the subduction zone[31] (Extended Data Fig. 1-2).

# References and Notes


1 Hinga, B. D. R. *Ring of Fire: An Encyclopedia of the Pacific Rim's Earthquakes, Tsunamis, and Volcanoes: An Encyclopedia of the Pacific Rim's Earthquakes, Tsunamis, and Volcanoes*. (ABC-CLIO, 2015).

2 Popa, R.-G., Bachmann, O. & Huber, C. Explosive or effusive style of volcanic eruption determined by magma storage conditions. *Nature Geoscience* **14**, 781-786, doi:10.1038/s41561-021-00827-9 (2021).

3 Allison, C. M., Roggensack, K. & Clarke, A. B. Highly explosive basaltic eruptions driven by CO2 exsolution. *Nature Communications* **12**, 217, doi:10.1038/s41467-020-20354-2 (2021).

4 Sheldrake, T. & Caricchi, L. Regional variability in the frequency and magnitude of large explosive volcanic eruptions. *Geology* **45**, 111-114, doi:10.1130/g38372.1 (2017).

5 Weber, G., Caricchi, L., Arce, J. L. & Schmitt, A. K. Determining the current size and state of subvolcanic magma reservoirs. *Nature Communications* **11**, 5477, doi:10.1038/s41467-020-19084-2 (2020).

6 Caricchi, L., Townsend, M., Rivalta, E. & Namiki, A. The build-up and triggers of volcanic eruptions. *Nature Reviews Earth & Environment* **2**, 458-476, doi:10.1038/s43017-021-00174-8 (2021).

7 Fierstein, J. & Hildreth, W. The plinian eruptions of 1912 at Novarupta, Katmai National Park, Alaska. *Bulletin of Volcanology* **54**, 646-684, doi:10.1007/BF00430778 (1992).

8 Self, S., Zhao, J.-X., Holasek, R. E., Torres, R. C. & King, A. J. The atmospheric impact of the 1991 Mount Pinatubo eruption. (1993).

9 Newhall, C. G. *et al. Eruptive History of Mount Pinatubo*. (Philippine Institute of Volcanology and Seismology; University of Washington Press, 1996).

10 Robock, A. Volcanic eruptions and climate. *Reviews of geophysics* **38**, 191-219 (2000).

11 Sun, S. s. & McDonough, W. F. Chemical and isotopic systematics of oceanic basalts: implications for mantle composition and processes. *Geological Society, London, Special Publications* **42**, 313-345, doi:10.1144/gsl.Sp.1989.042.01.19 (1989).

12 Adam, V., Mike, C., Joshua, S. & Lauren, D. *Hunga Tonga-Hunga Ha'apai Erupts*, 2022).

13 Cronin, S. *Why the volcanic eruption in Tonga was so violent, and what to expect next*, 2022).

14 S. J. Cronin *et al. New Volcanic Island Unveils Explosive Past*. Vol. 26 June (EOS Science News by AGU, 2017).

15 Plank, T. & Langmuir, C. H. The chemical composition of subducting sediment and its consequences for the crust and mantle. *Chemical geology* **145**, 325-394 (1998).

16 Amante, C. & Eakins, B. ETOPO1 1 Arc-Minute Global Relief Model: procedures, data sources and analysis. doi:10.7289/V5C8276M (2009).

17 Luyendyk, B. P. *calcite compensation depth*. Vol. 2009 (Encyclopedia Britannica, 2009).

18 Plank, T. & Manning, C. E. Subducting carbon. *Nature* **574**, 343-352, doi:10.1038/s41586-019-1643-z (2019).

19 Koppers, A. A. P., Duncan, R. A. & Steinberger, B. Implications of a nonlinear 40Ar/39Ar age progression along the Louisville seamount trail for models of fixed and moving hot spots. *Geochemistry, Geophysics, Geosystems* **5**, Q06L02, doi:

https://doi.org/10.1029/2003GC000671 (2004).

20 Tejada, M. L. G., Mahoney, J. J., Neal, C. R., Duncan, R. A. & Petterson, M. G. Basement Geochemistry and Geochronology of Central Malaita, Solomon Islands, with Implications for the Origin and Evolution of the Ontong Java Plateau. *Journal of Petrology* **43**, 449-484, doi:10.1093/petrology/43.3.449 (2002).

21 Taylor, B. The single largest oceanic plateau: Ontong Java–Manihiki–Hikurangi. *Earth and Planetary Science Letters* **241**, 372-380, doi:https://doi.org/10.1016/j.epsl.2005.11.049 (2006).

22 Worthington, T. J., Hekinian, R., Stoffers, P., Kuhn, T. & Hauff, F. Osbourn Trough: Structure, geochemistry and implications of a mid-Cretaceous paleospreading ridge in the South Pacific. *Earth and Planetary Science Letters* **245**, 685-701, doi:https://doi.org/10.1016/j.epsl.2006.03.018 (2006).

23 Sun, W., Zhang, L. & Liu, X. The rotation of the Pacific Plate induced by the Ontong Java large igneous. *Journal of Earth Science*, doi:https://doi.org/10.1007/s12583-021-1582-0 (2022).

24 Seton, M. *et al.* Global continental and ocean basin reconstructions since 200Ma. *Earth-Science Reviews* **113**, 212-270, doi:10.1016/j.earscirev.2012.03.002 (2012).

25 Ruellan, E., Delteil, J., Wright, I. & Matsumoto, T. From rifting to active spreading in the Lau Basin – Havre Trough backarc system (SW Pacific): Locking/unlocking induced by seamount chain subduction. *Geochemistry, Geophysics, Geosystems* **4**, doi:https://doi.org/10.1029/2001GC000261 (2003).

26 Benz, H. M. *et al.* Seismicity of the Earth 1900-2010 eastern margin of the Australia plate. Report No. 2331-1258, (US Geological Survey, 2011).

27 Koppers, A. *et al.* Louisville Seamount Trail: implications for geodynamic mantle flow models and the geochemical evolution of primary hotspots. *IODP Prelimary Report*, doi:10.2204/iodp.pr.330.2011 (2011).

28 Burke, K. D. *et al.* Pliocene and Eocene provide best analogs for near-future climates. *Proceedings of the National Academy of Sciences* **115**, 13288-13293, doi:10.1073/pnas.1809600115 (2018).

29 Buchs, D. M., Williams, R., Sano, S.-i. & Wright, V. P. Non-Hawaiian lithostratigraphy of Louisville seamounts and the formation of high-latitude oceanic islands and guyots. *Journal of Volcanology and Geothermal Research* **356**, 1-23, doi:https://doi.org/10.1016/j.jvolgeores.2017.12.019 (2018).

30 Dasgupta, R. Ingassing, storage, and outgassing of terrestrial carbon through geologic time. *Reviews in Mineralogy and Geochemistry* **75**, 183-229 (2013).

31 Chen, W. & Brudzinski, M. R. Evidence for a Large-Scale Remnant of Subducted Lithosphere Beneath Fiji. *Science* **292**, 2475-2479, doi:doi:10.1126/science.292.5526.2475 (2001).

32 Zhan, M., Sun, W., Ling, M. X. & Li, H. Huangyan ridge subduction and formation of porphyry Cu-Au deposits in Luzon. *Acta Petrologica Sinica* **31**, 2101-2114 (2015).

33 Yang, T. F. *et al.* A double island arc between Taiwan and Luzon: consequence of ridge subduction. *Tectonophysics* **258**, 85-101, doi:https://doi.org/10.1016/0040-1951(95)00180-8 (1996).

34 Briais, A., Patriat, P. & Tapponnier, P. Updated interpretation of magnetic anomalies and

seafloor spreading stages in the south China Sea: Implications for the Tertiary tectonics of Southeast Asia. *Journal of Geophysical Research: Solid Earth* **98**, 6299-6328, doi:10.1029/92jb02280 (1993).

35 Bândă, N. *et al.* The effect of stratospheric sulfur from Mount Pinatubo on tropospheric oxidizing capacity and methane. *Journal of Geophysical Research: Atmospheres* **120**, 1202-1220, doi:https://doi.org/10.1002/2014JD022137 (2015).

36 Oman, L., Robock, A., Stenchikov, G., Schmidt, G. A. & Ruedy, R. Climatic response to high-latitude volcanic eruptions. *Journal of Geophysical Research: Atmospheres* **110** (2005).

37 Plank, T. The Chemical Composition of Subducting Sediments. *Treatise on Geochemistry*, 607-629, doi:10.1016/b978-0-08-095975-7.00319-3 (2014).

38 Barker, P. & Kennett, J. Leg 113. *Proceedings of the Ocean Drilling Program Initial Reports of Leg* **113**, 785 (1988).

39 Gou, T., Zhao, D., Huang, Z. & Wang, L. Aseismic Deep Slab and Mantle Flow Beneath Alaska: Insight From Anisotropic Tomography. *Journal of Geophysical Research: Solid Earth* **124**, 1700-1724, doi:https://doi.org/10.1029/2018JB016639 (2019).

40 Seno, T., Stein, S. & Gripp, A. E. A model for the motion of the Philippine Sea Plate consistent with NUVEL-1 and geological data. *Journal of Geophysical Research: Solid Earth* **98**, 17941-17948, doi:https://doi.org/10.1029/93JB00782 (1993).

41 Kaneko, K., Mishiro, K. & Tatsumi, Y. Control of Volcanic Activity by Crustal Structure: Inference from the Izu-Bonin-Mariana and Northeast Japan Arcs. *Geophysical Research Letters* **46**, 12968-12976, doi:https://doi.org/10.1029/2019GL084554 (2019).

42 Macdonald, K. C. in *Encyclopedia of Ocean Sciences (Third Edition)* (eds J. Kirk Cochran, Henry J. Bokuniewicz, & Patricia L. Yager) 405-419 (Academic Press, 2019).

43 Kinoshita, S. M., Igarashi, T., Aoki, Y. & Takeo, M. Imaging crust and upper mantle beneath Mount Fuji, Japan, by receiver functions. *Journal of Geophysical Research: Solid Earth* **120**, 3240-3254, doi:https://doi.org/10.1002/2014JB011522 (2015).

44 Engdahl, E. R., van der Hilst, R. & Buland, R. Global teleseismic earthquake relocation with improved travel times and procedures for depth determination. *Bulletin of the Seismological Society of America* **88**, 722-743, doi:10.1785/bssa0880030722 (1998).

45 Venzke, E. Global Volcanism Program. Volcanoes of the World, v. 4.9. 1 (17 Sep 2020). (2013).

46 Minnett, R., Staudigel, H. & Koppers, A. A. Seamount Catalong: Seamount Morphology, Maps, and Data Files. *Earth Reference Data and Models* (2010).

47 Bardach, J. E., Cotter, C. H. & Morgan, J. R. *Pacific Ocean*. Vol. 2022 (Encyclopedia Britannica, 2021).

48 Aakanksha, G. *et al. Tonga Trench*. Vol. 2022 (Encyclopedia Britannica, 2018).

49 Tozer, B. *et al.* Global Bathymetry and Topography at 15 Arc Sec: SRTM15+. *Earth and Space Science* **6**, 1847-1864, doi:https://doi.org/10.1029/2019EA000658 (2019).

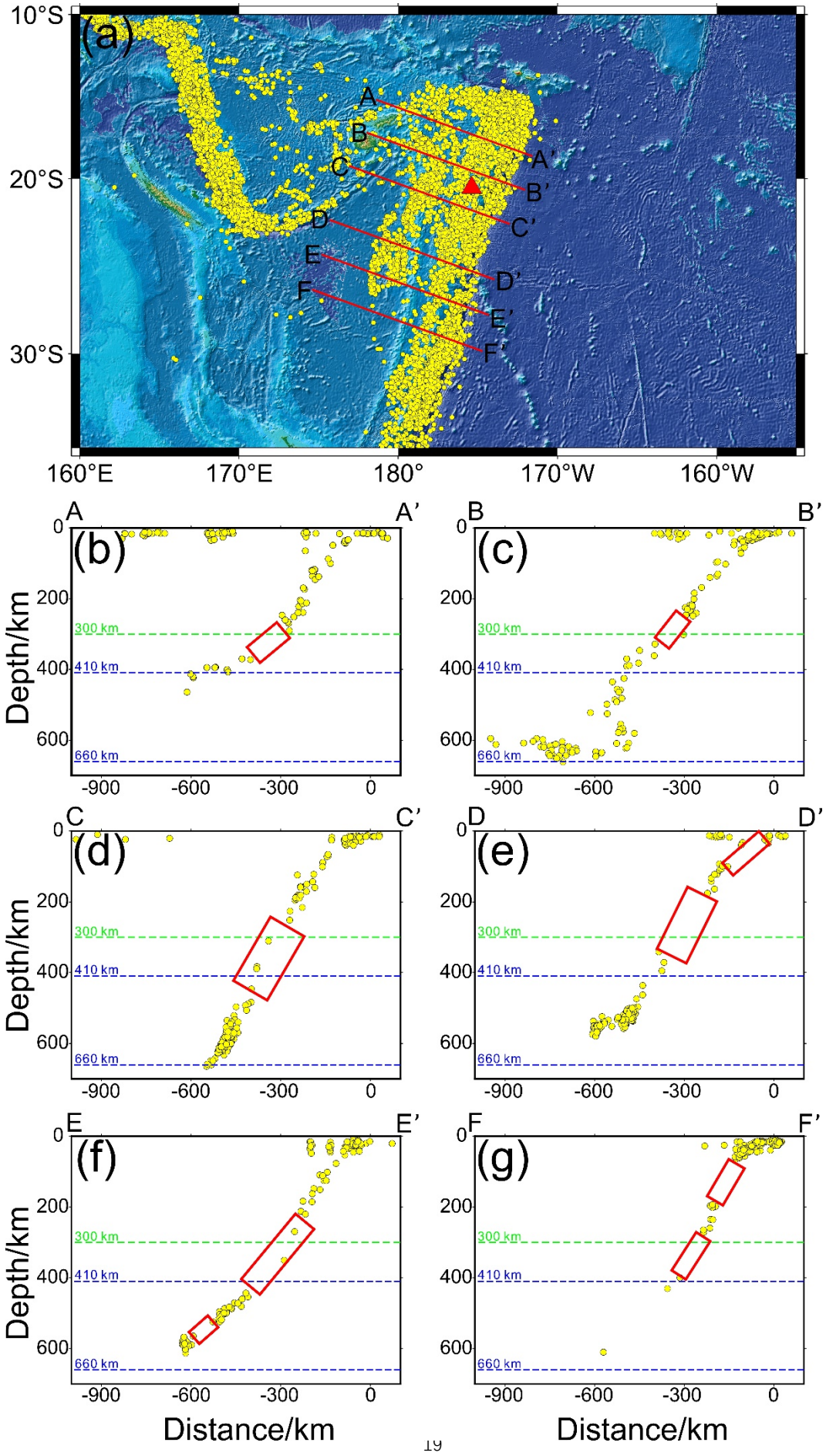
(a)
10°S
20°S
30°S
160°E
170°E
180°
170°W
160°W
A
A'
B
B'
C
C'
D
D'
E
E'
F
F'
(b)
(c)
(d)
(e)
(f)
(g)
Depth/km
Distance/km
0
200
400
600
300 km
410 km
660 km
-900
-600
-300
0

**Extended Data Figure 1 | Slab tearing under the Tonga-Kermadec subduction zone.** (a) Seismicity with $M_b > 5$ between 1964 and 2018 from the ISC-EHB catalog[44]. Yellow circles indicate the earthquake epicenters. Red triangle represents the location of the Hunga Tonga-Hunga Ha'apai volcano. Red lines are labeled cross sections of seismicity (Extended Data Fig. 1b-g). (b)-(g) Seismicity distributions of along the cross section in (a). Yellow circles represent the earthquake epicenters. Green and blue dashed lines indicate 300, 410 and 660 km, respectively. Red squares represent the location where slab tearing is likely to occur.

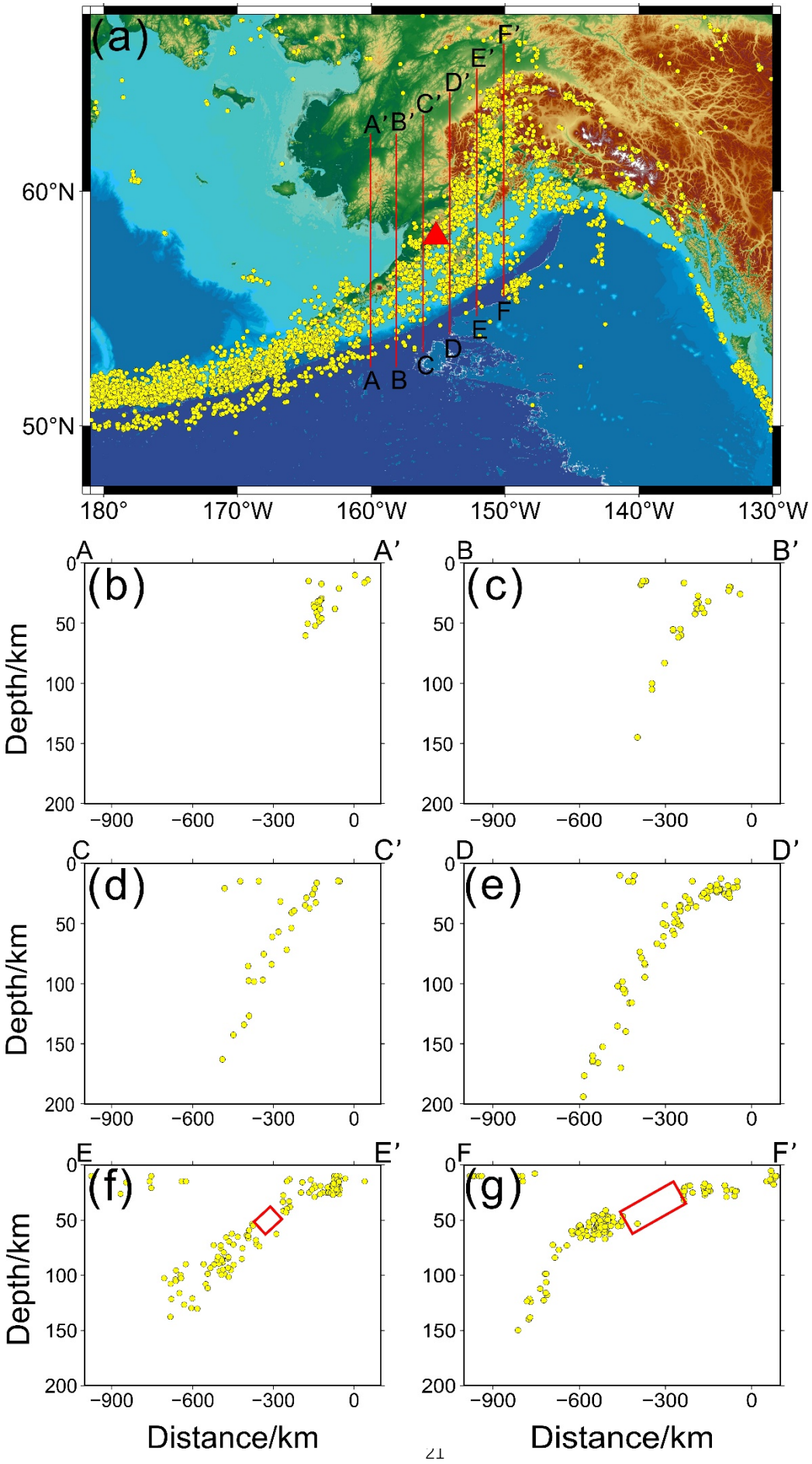
(a)
A'
B'
C'
D'
E'
F'
A
B
C
D
E
F
60°N
50°N
180°
170°W
160°W
150°W
140°W
130°W
(b)
(c)
(d)
(e)
(f)
(g)
Depth/km
Distance/km
0
50
100
150
200
−900
−600
−300
0

**Extended Data Figure 2 | Slab tearing under the Aleutian- Alaska subduction zone.** (a) Seismicity with $M_b > 4$ between 1964 and 2018 from the ISC-EHB catalog[44]. Yellow circles indicate the earthquake epicenters. Red triangle represents the location of the Novarupta volcano. Red lines are labeled cross sections of seismicity (Extended Data Figure. 2b-g). (b)-(g) Seismicity distributions of along the cross section in (a). Yellow circles represent the earthquake epicenters. Red squares represent the location where slab tearing is likely to occur.